

DUAL AND TRIPLE FEEDING FOR FULL-WAVE DIPOLE ANTENNA

KHEDHER A. HMOOD

UNIVERSITI SAINS MALAYSIA

2007

DUAL AND TRIPLE FEEDING FOR FULL-WAVE DIPOLE ANTENNA

by

KHEDHER A. HMOOD

Thesis submitted in fulfillment of the requirements
for degree of Doctor of Philosophy

January, 2007

Acknowledgments

First, I am highly thankful and indebted to Allah Subhanahu Wata'ala for providing me peace of mind, ability and will to complete this work.

I am very grateful to Prof Syed Idris Syed Hassan, who has served many years as my supervisor for my study towards PhD. Prof Syed Idris provided invaluable guidance and support throughout the work on this thesis. Without his support and patience I would not have completed my doctoral degree.

Peace and Rahmah be upon my father Abood Hmood Al-Jebouri. He had inspired me to strive for excellence. May Allah bestow him with Al Firdaus. I am grateful to my mother for her spiritual support and Dua'a.

I would like to express my gratitude to The Acting Dean of School of Electrical & Electronic Engineering, Dr Mohd Rizal Arshad, for constant encouragement during my study. I would like to thank all the academic, administrative and technical staff at the School of Electrical and Electronic Engineering for their kind support and help. I would like to thank my adorable wife Shahnail Asmar Binti Saaid, and her family and my beloved daughter Mariah AL-Qubtiyah for their patience and unflinching support. I am also thankful to all my brothers and sisters; namely, Mohsen, Khairiah, Safiah, Hasnah and, Ali for their caring and dua'a.

I would like to thank my friends Dr Zul, Dr Yousif, Ali Aljubouri, Farooqi, Anwar, Anas, Amer, Battah, Jawad, Saeed Ajjaj, Khalid, Muatasem, Bashsar, Wael, Khalid Al Aithawi, Basim, Othman Alhanbali, Saleh, Yazeed and Salah Darwash for their assistance and affection.

Khedher Abood Hmood Al Jeboury

TABLE OF CONTENTS

	Pg.No
ACKNOWLEDGEMENTS	i
TABLE OF CONTENTS	ii
LIST OF FIGURES	v
LIST OF TABLES	ix
ABSTRAK	x
ABSTRACT	xii
CHAPTER 1: INTRODUCTION	1
1.1 Introduction	1
1.2 Motivations	2
1.3 Goals and Objectives	2
1.4 Thesis Organization	4
CHAPTER 2: LITERATURE REVIEW	5
2.1 Current Distribution on Linear Antenna	5
2.2 Feed Mechanisms for Full -Wave Dipole Antenna	20
2.2.1 Center- Fed Dipole Antenna	20
2.2.2 Off-Center Fed Dipole Antenna	24
2.2.3 End-Fed Full-Wave Dipole Antenna	26
CHAPTER 3: ANTENNA CONSTRUCTION AND IMPEDANCE MATCHING	34
3.1 Introduction	34
3.2 Symmetrical Dual Feeding Antennas	34
3.3 Asymmetrical Dual Feeding Antenna	35
3.4 Triple Feeding Full-Wave Antenna	35
3.5 Input Impedance Measurements	43

3.6	Matching for Dual and Triple Feeding Antenna	46
	3.6.1 Matching Techniques	47
	3.6.1.1 Matching Circuit for Symmetrical Dual Feeding	49
	3.6.1.2 Matching Circuit for Asymmetrical Dual Feeding	52
	3.6.1.3 Matching Circuit for Triple Feeding	55
	CHAPTER 4: METHODOLOGY & MEASUREMENTS TECHNIQUE	59
4.1	Introduction	59
4.2	Current Distribution	60
	4.2.1 Measurement Method	60
4.3	Radiation Pattern	63
	4.3.1 Measurement Method	64
	4.3.2 Far-Field Ranges	65
4.4	Gain	69
	4.4.1 Gain Measurement	69
	CHAPTER 5: RESULTS AND DISSCUSION	72
5.1	Introduction	72
5.2	Results of Current Distribution	72
	5.2.1 Symmetrical Dual Feeding	72
	5.2.2 Asymmetrical Dual Feeding	74
	5.2.3 Triple Feeding	77
5.3	Discussion on Current Distribution	79
	5.3.1 Symmetrical Dual Feeding	81
	5.3.2 Symmetrical Dual Feeding	87
	5.3.3 Triple Feeding	92

5.4	Derivations and Theoretical Development of the Pattern	96
5.4.1	Antenna A1	97
5.4.2	Antenna A2	100
5.4.3	Antenna B1	102
5.4.4	Antenna B2	104
5.4.5	Antenna C1	107
5.4.6	Antenna C2	108
5.4.7	Antenna C3	110
5.5	Theoretical Development of the Gain	112
5.5.1	Gain of Antenna A1	112
5.5.2	Gain of Antenna A2	115
5.5.3	Gain of Antenna B1	116
5.5.4	Gain of Antenna B2	117
5.5.5	Gain of Antenna C1	118
5.5.6	Gain of Antenna C2	120
5.5.7	Gain of Antenna C3	120
5.5.8	Discussion	121
	CHAPTER 6: CONCLUSIONS AND FUTURE WORK	124
6.1	Conclusions	124
6.2	Future Work	127
	REFERENCES	128
	APPENDICES	139
	APPENDIX A	140
	APPENDIX B	147

LIST OF FIGURES

Figure 2.1	Geometry of the Center- Fed Dipole	7
Figure 2.2	Current distribution on wire antenna with different lengths	10
Figure 2.3	Thin wire model for linear antenna (Orfanidis 2004)	13
Figure 2.4	Current distribution on linear antenna (Orfanidis 2004)	14
Figure 2.5	Geometry of Cylindrical Dipole Antenna	15
Figure 2.6	Comparison of real and imaginary current distributions on full-wave unloaded antenna calculated by King's approximation and matrix methods (Rusch, 1959)	18
Figure 2.7	(A) a center-fed dipole antenna, (B) The Current Distribution along the length of the Dipole	21
Figure 2.8	Dipole antenna with trap	23
Figure 2.9	Current distributions on wire antenna with traps	23
Figure 2.10	Current distributions on Full-Wave Antenna (Vinoy et al., 2001)	26
Figure 2.11	The current distribution of End-Fed Full-Wave Out-Of-Phase Dipole Antenna	28
Figure 2.12	Current distribution on End-Fed Full-Wave In Phase Dipole Antenna	28
Figure 2.13(A)	Current vector alignment and off feed point location (Gosalia, 2004)	29
Figure 2.13(B)	Simulated Current magnitude and phase distribution on off center-fed wire (Gosalia, 2004)	29
Figure 2.14(A)	Current vector alignment and Center-Fed point Location with phase reversal (Gosalia, 2004)	30
Figure 2.14(B)	Simulated Current magnitude and phase distribution of Center-Fed wire with center phase reversal (Gosalia, 2004)	30
Figure 2.15	Radiation Pattern of Half Wave Dipole	33

Figure 2.16	Current Distribution and the Radiation Pattern of Full-Wavelength Antenna	33
Figure 3.1	Feeding arrangements for symmetrical Dual Feeding in Phase Antenna	36
Figure 3.2	Feeding arrangements for Symmetrical Dual Feeding Out of Phase Antenna	37
Figure 3.3	Feeding arrangements for Asymmetrical Dual Feeding in Phase Antenna	38
Figure 3.4	Feeding arrangements for Asymmetrical Dual Feeding Out of Phase Antenna	39
Figure 3.5	Feeding Arrangements for Triple Feeding Full Wave Antenna	40
Figure 3.6	Feeding Arrangements for Triple Feeding Full Wave Antenna	41
Figure 3.7	Feeding Arrangements for Triple Feeding Full Wave Antenna	42
Figure 3.8	Measurements setup for measuring the input impedance	45
Figure 3.9	Balun (balanced-to-unbalanced transformer)	46
Figure 3.10	Matching Transformer Sections for Symmetrical Dual Feeding	50
Figure 3.11	Measured and Simulated SWR vs. frequency for Antenna A1	51
Figure 3.12	Measured and Simulated SWR vs. frequency for Antenna A2	51
Figure 3.13	Matching transformer sections for Asymmetrical Dual Feeding	53
Figure 3.14	Measured and Simulated SWR vs. frequency for Antenna B1	54
Figure 3.15	Measured and Simulated SWR vs. frequency for Antenna B2	54
Figure 3.16	Matching Circuit for Triple Feeding Full Wave Dipole Antenna.	55

Figure 3.17	Measured and Simulated SWR vs. frequency for Antenna C1	56
Figure 3.18	Measured and Simulated SWR vs. frequency for Antenna C2	56
Figure 3.19	Measured and Simulated SWR vs. frequency for Antenna C3	57
Figure 4.1	Measurements of current distribution using two shielded loops	61
Figure 4.2	Radiation Pattern Measurement Setup	65
Figure 4.3	Far Field Measurements Setup using IEEE Standard	68
Figure 4.4	Standard Reflection Range of Measurements Setup using IEEE Standard	68
Figure 5.1	Measured and predicted current distribution for Antenna A1	73
Figure 5.2	Measured and predicted current distribution for Antenna A2	74
Figure 5.3	Measured and predicted current distribution for Antenna B1	75
Figure 5.4	Measured and predicted current distribution for Antenna B2	76
Figure 5.5	Measured and predicted current distribution for Antenna C1	78
Figure 5.6	Measured and predicted current distribution for Antenna C2	78
Figure 5.7	Measured and predicted current distribution for Antenna C3	79
Figure 5.8	Comparison between the simulated currents, and predicted current of Antenna A1	84
Figure 5.9	Comparison between the simulated currents, and predicted current of Antenna A1	85
Figure 5.10	Comparison between the simulated currents, and predicted current of Antenna A1	85

Figure 5.11	Comparison between the simulated currents, and predicted current of Antenna A1	86
Figure 5.12	Comparison between the simulated currents, and predicted current of Antenna B1, B2	90
Figure 5.13	Comparison between the simulated currents, and predicted current of Antenna B1, B2	91
Figure 5.14	Comparison between the simulated currents, and predicted current of Antenna B1, B2	91
Figure 5.15	Comparison between simulated currents, and predicted current of Antenna B1, B2	92
Figure 5.16	Predicted Current Distribution for Antenna C1, C2, C3	94
Figure 5.17	Simulated current distribution for full wave antenna	95
Figure 5.18	Coordinate System Used with Antennas	96
Figure 5.19	Radiation Pattern of Antenna A1	99
Figure 5.20	Radiation Pattern of Antenna A2	101
Figure 5.21	Radiation Pattern of Antenna B1	104
Figure 5.22	Radiation Pattern of Antenna B2	106
Figure 5.23	Radiation Pattern of Antenna C1	108
Figure 5.24	Radiation Pattern of Antenna C2	109
Figure 5.25	Radiation Pattern of Antenna C3	111

LIST OF TABLES

Table 3.1	A specifications and References of full wave dipole antennas	43
Table 3.2	LC matching parameters, and dimensions of substrates for seven full- wave dipole antennas	49
Table 5.1	Measured and theoretical parameters of Full wave antenna	123

ANTENA DWIKUTUB GELOMBANG PENUH DENGAN DUA DAN TIGA SUAPAN

ABSTRAK

Tesis ini menfokus kepada pembangunan teknik baru untuk suapan antenna dwikutub gelombang penuh. Terdapat tujuh cara suapan dalam kajian ini, empat cara untuk dua suapan dan tiga cara untuk tiga suapan. Antena telah dibina menggunakan batang aluminium berkeratan rentas bentuk-U dengan panjang, lebar, tinggi berdimensi 100 X 2.5 X 2 cm. Pemadanan antenna pula telah menggunakan balun dan mikrostrip. Mula-mula taburan arus pada antenna diukur, dan diikuti dengan sukatan parameter antenna yang lain seperti gandaan, corak sinaran dan galangan antenna. Daripada arus ini, tujuh persamaan taburan arus telah dirumuskan. Ia kemudiannya digunakan untuk menentukan corak sinaran dan gandaan antenna tersebut. Akhir sekali nilai-nilai yang diperolehi secara teori dan pengukuran dibandingkan untuk menentukan kesahihan persamaan yang dibangunkan. Disamping itu, program perisian MATLAB yang telah dibangunkan diubahsuai dan digunakan untuk menyelakukan galangan masukan, gandaan dan corak sinaran kemudian dibandingkan dengan nilai-nilai parameter yang diperolehi secara amali. Hubungan yang berkait rapat telah didapati antara pengukuran dan keputusan simulasi. Ia menunjukkan teknik dua suapan bersimetri secara teori boleh mencapai gandaan 3.8dBi, dan dua suapan tak simetri mencapai gandaan 2.4dBi. Manakala teknik tiga suapan pula boleh menghasilkan prestasi antenna yang baik secara keseluruhan, dengan gandaan 6.7dBi, corak sinaran dengan lebarjalur yang kecil dan galangan masukan 50Ω selepas pemadanan. Sedikit perselisihan didapati di dalam beberapa kes merujuk kepada taburan arus

dibandingkan dengan penghampiran King dan Hallen yang mungkin disebabkan ketebalan dawai dan ralat pengukuran.

DUAL AND TRIPLE FEEDING FOR FULL WAVE DIPOLE ANTENNA

ABSTRACT

This thesis is focused on the development of a new full-wave dipole antenna feeding technique. Seven such techniques of feeding were tested in the study, in which, four were used with dual feeding and three with triple feeding. The antennas were constructed using channel-shaped aluminum section with length, width and height of 100 X 2.5 X 2 cm, respectively. The antennas were matched using balun and microstrip circuits. Initially, the current distribution was measured, followed by the measurement of parameters of antenna such as gain, radiation patterns and input impedance. Based on these observations seven Equations for current distribution were eventually formulated. These Equations were then used to compute the values of the same parameters of the antenna. Finally, the values of parameters obtained practically and theoretically were compared to analyze the validity of the developed Equations. Besides, the already developed Matlab based software program was modified and employed to simulate the input impedance, gain and radiation pattern and compared with the values of parameters obtained experimentally. A good agreement was observed between the measured, computed and simulated results. It is shown that a symmetrical dual feeding and asymmetrical dual feeding techniques, theoretically achieved a gain of 3.8 dBi, and 2.4 dBi respectively. The triple feeding provided an overall best performance, with gain 6.7dBi, radiation pattern with narrow beam width and input impedance of 50 Ω . Slight discrepancy was observed in some cases regarding the current distribution when compared

to the King's and Hallen's approximations, and that can be attributed to the thickness of the wire antenna and the error of measurement.

CHAPTER 1

INTRODUCTION

1.1 Introduction

For a true harmonic operation, it is necessary that power is to be fed into the antenna is at an appropriate point. Mei (1965); Mille (1975); Li (1996); Rogers (1997) have shown that there are two methods that result in the proper current distribution. If the source of power is connected to the antenna at one end of the full-wave, the direction of current flow is reversed in alternate $1/2 \lambda$ section, or if the power is inserted at the center of the full wave dipole antenna. Caswell & Davis (1999) have shown that for harmonic operation, the antenna should be fed either at the end or at the center. If the feed point is at the end of the antenna, the current distribution would be different than that expected on a properly fed harmonic antenna (end fed).

In this study a full wave dipole antenna was to be fed by various methods. These methods can be classified into three categories; namely, symmetrical dual feeding, asymmetrical dual feeding and symmetrical triple feeding. Variation in the current distribution is dependent on the feed location and the feed point polarity. The current distributions were measured, modeled and formulated whose parameters were deduced from the measured current distribution by applying the current distribution data in models as derived by IEEE standard. According to Takamizawa, et al. (2001), it is difficult to apply directly the measured data in the forms derived by the same authors.

1.2 Motivations

The full-wave consists mainly of one feeding point connected to the antenna and for center single fed, the antenna introduces excessively high impedance due to the low current at the terminal (Idris et al., 1994; Balanis, 1997; Stutzman & Gary, 1998). The radiation resistance of the antenna is 193.9Ω (Kraus, 1950; Maclean, 1986; Idris, et al., 1994), which is not suited for standard coaxial cable (Abdelsayed, et al., 2005), and the gain of the center fed is -0.2 dBi (Idris et al., 1999). For off single center fed, it was reported that as the feed point moves away from the center, the input impedance increases to infinity. However, the off-center feed is unsymmetrical and can lead to undesirable phase reversal in the antenna (Shen & Robert, 2001; Bandler, et al., 2002). Idris et al. (1994) has shown that the gain of the off single fed is 0.5 dBi while the input impedance is 180Ω . In this study, it was found that the full-wave antenna offers a high gain by devising the feeding and applying multi feeding instead of one. Novel design methodologies and implementation techniques for full wave antennas with dual and triple feeding are studied.

1.3 Goals and Objectives

The objectives of this thesis are

- a) To design and construct multi fed full-wave dipole antennas including matching.
- b) To investigate experimentally the quantitative relationship between the current distribution to the feeding modifications and the polarity of the feeding.

- c) To obtain the expressions for current distribution, and formulate the equations of the current distribution using curve fitting and trial and error methods in order to propose an algorithm for the current distribution.
- d) To deduce the parameters of the full wave antenna such as radiation pattern, gain and input impedance based on the data of the formulated current distribution in standard forms so as to be able to predict theoretically the deduced parameters.
- e) To measure and compare the radiation pattern, gain, and input impedance parameters of multi fed full wave dipole antenna obtained from the experimental with the formulated parameters.

In order to achieve these objectives, the current distribution is expressed in terms of the current and its derivative with the measurement point-dependent coefficients. Several dipole antennas with two and three feeding have been fabricated from the U-shape aluminum with loop antenna used to measure the current distribution. The equations of current are formulated using curve fitting and trial and error. They were developed to give seven equations with respect to the seven types of full wave antenna. These equations were used to deduce the parameters of the antenna. Finally the theoretical results were compared with those obtained experimentally. These models can be applied to any general form of full-wave antenna of any size and configuration. Three types of source impedance matching conditions for multi fed full wave antennas were investigated. The gain, radiation pattern, and input impedance were measured and compared with the developed models.

1.4 Thesis Organization

The second Chapter of this dissertation reviews the background literatures related to the present work specifically the current distribution on linear antenna and single feeding techniques including feeding effects. The advantages and disadvantages of existing techniques will be discussed. In Chapter 3, the construction of seven full-waves dipole antennas were described with different type of feeding followed by the investigation of the impedance matching of sources to the full wave antenna. In Chapter 4, a conventional method technique was described to measure the current distribution, radiation pattern, and gain on the full wave dipole antennas. In Chapter 5 the derivation and validity of the equations of the measured current distribution for the seven antennas was presented, a conventional full wave analysis technique used for deriving the radiation pattern and gain was discussed. This technique was sufficient in predicting the full wave radiation patterns. Theoretical development of the radiation pattern is presented in this Chapter, and the measurement results of the gain and the theoretical development of the gain are presented. The conclusions and recommendations for future work are presented in Chapter 6.

CHAPTER 2

LITERATURE REVIEW

2.1 Current Distribution on Linear Antenna

Most antennas reversibly link radiation fields to currents flowing in wires at frequencies ranging from sub-audio through the far-infrared region. The current distribution along a linear, receiving antenna feeding may be found using the theorem of reciprocity and the data of the current distribution of an identical transmitting antenna. If prior knowledge of the transmitting antenna current distribution is lacking, the current distribution of a receiving antenna with a matched load can be derived from the incident electric field and both approaches yield similar results (Georgieva, 2002).

King (1956); King & Harrison (1969); Davis (1995) stated that the current distribution along a receiving dipole antenna depends greatly on the load Z_L , and they concluded that the simple sinusoidal current distribution approximation is valid only when the load impedance is small or is equal to the complex conjugate of the antenna feed-point impedance.

The current distributions have maximum values at the feed points. However, when the load impedance is high, the dipole antenna behaves more like a two-element collinear scattering array. For this case, the current at the feed points decreases significantly, and the simple sinusoidal approximation for the current distribution is no longer valid (Collin, 1960; Edminister, 1993; Khamas, 1997; Khamas et al., 1997; Werner, 1998; Best 2002).

For linear antennas, the z-axis has been chosen to be along the direction of the antenna. Assuming an infinitely thin antenna, the current density $J(r)$ will have the form

$$J(r) = \hat{z} I(z) \delta(x) \delta(y) \quad (\text{Thin linear antenna}) \quad 2.1$$

Where $I(z)$ is the current distribution along the antenna element as it was reported by many researchers (Hallen, 1938; King, 1949; Mei, 1965; King & T.Wu, 1967; Miller, 1969; Mittra & Lee 1971; Taylor & Wilton, 1972; Balanis, 1982; Hassan, 1987; Idris et al., 1994; Werner, 1998). They showed that the current distribution for a linear antenna has different forms

$$I(z) = IL\delta(z) \quad \text{Hertzian dipole} \quad 2.2$$

$$I(z) = I \quad \text{Uniform linear element} \quad 2.3$$

$$I(z) = I(L - 2|z|/L) \quad \text{Small linear dipole} \quad 2.4$$

$$I(z) = I \sin \beta \left(\frac{L}{2} - |z| \right) \quad \text{Standing wave antenna} \quad 2.5$$

$$I(z) = I \cos \beta z \quad \text{Half wave Dipole} \quad 2.6$$

$$I(z) = I e^{-j\beta z} \quad \text{Traveling wave antenna} \quad 2.7$$

Where $I(z)$ is the current at any point on the antenna at z direction, β is the phase constant, $\beta = \frac{2\pi}{\lambda}$, λ is wavelength in meter, L is the length of the antenna element and the expressions are assumed to be valid for $-\frac{L}{2} \leq z \leq \frac{L}{2}$, so that the antenna element straddles the x y -plane.

A very practical antenna is the center-fed standing-wave antenna, and in particular, the half-wave dipole whose length is $L = \frac{\lambda}{2}$, where λ is wavelength in meter. The current distribution along the antenna length is assumed to be a standing wave, much like the case of an open-ended parallel wire transmission line. Similarly, as suggested in Figure 2.1, the center-fed dipole may be thought of as an open-ended transmission line whose ends have been bent up and down (Ivanova, 1997).

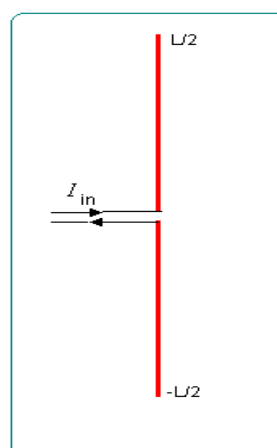


Figure 2.1: Geometry of the Center- Fed Dipole

Orfanidis (2004) has shown that for a general dipole of length L , the current at the input terminals of the antenna is not necessarily equal to the peak amplitude. Setting the variable $z = 0$ in Equation (2.5) yields

$$I_{in} = I(0) = \sin \beta \left(\frac{L}{2} \right) \quad 2.8$$

Where I_{in} is the input current, and L is the length of the antenna, β is the phase constant, $\beta = \frac{2\pi}{\lambda}$ and λ is wavelength in meter.

When L is a half-multiple of the wave length λ , element the input and peak currents are equal and the two definitions of the radiation resistance are the same. But when L is a multiple of λ , Equation 2.8 gives zero for the input current, which would imply an infinite input resistance R_{in} (Georgieva, 2002; Orfanidis, 2004).

In practice, the current distribution is only approximately sinusoidal and the input current is not exactly zero. The z-component of radiation vector $F_z(\theta)$ is depicted in Equation 2.9 (Schelkunoff, 1952; King; King et al. 1968; Werner, 1996; Georgieva, 2002).

$$F_z(\theta) = \int_{-\frac{L}{2}}^{\frac{L}{2}} I(z) \sin \beta \left(\frac{L}{2} - |z| \right) e^{j\beta z \cos \theta} dz = \frac{2L}{\beta} \frac{\cos \left(\frac{\beta L}{2} \cos \theta \right) - \cos \left(\frac{\beta L}{2} \right)}{\sin^2 \theta} \quad 2.9$$

Where $I(z)$ is the current at any point on the antenna at z direction, β is the phase constant, $\beta = \frac{2\pi}{\lambda}$, λ is wavelength in meter, L is the length of the antenna element and the expressions are assumed to be valid for $-\frac{L}{2} \leq z \leq \frac{L}{2}$, so that the antenna element straddles the x y -plane.

The current distributions on various dipoles were plotted together with the antenna, which was used to generate them as shown in Figure 2.2. The sinusoidal curves superimposed on the antenna indicated the intensity of the current on the wire, that is, the value of the curve at point z is the current value on the wire at the same point (Kraus, 1988; Stutzman et al., 1995). The current at the ends of the antenna was zero because when a charge reaches the end of the antenna and is reflected, the direction of flowing current reverses. The next charge just reaches the end of the antenna, so two currents of essentially the same amplitude, but flowing in opposite directions exist at that point on the wire. The resultant current at the end of the antenna is therefore zero (Stutzman et al., 1995; Balanis, 1997; Takamizawa, 2001). Caron (1999) and Nikolova (2005) stated, if there is reflection from the end of a wire, the number of standing waves on the wire is equal to the length of the wire in half wavelengths. Thus, if the wire is two half-waves long, there are two standing waves; if three half-waves long, three standing waves, and so on. These longer wires, each multiples of $1/2 \lambda$ long, are therefore also resonant at the same frequency as the single $1/2 \lambda$ wire.

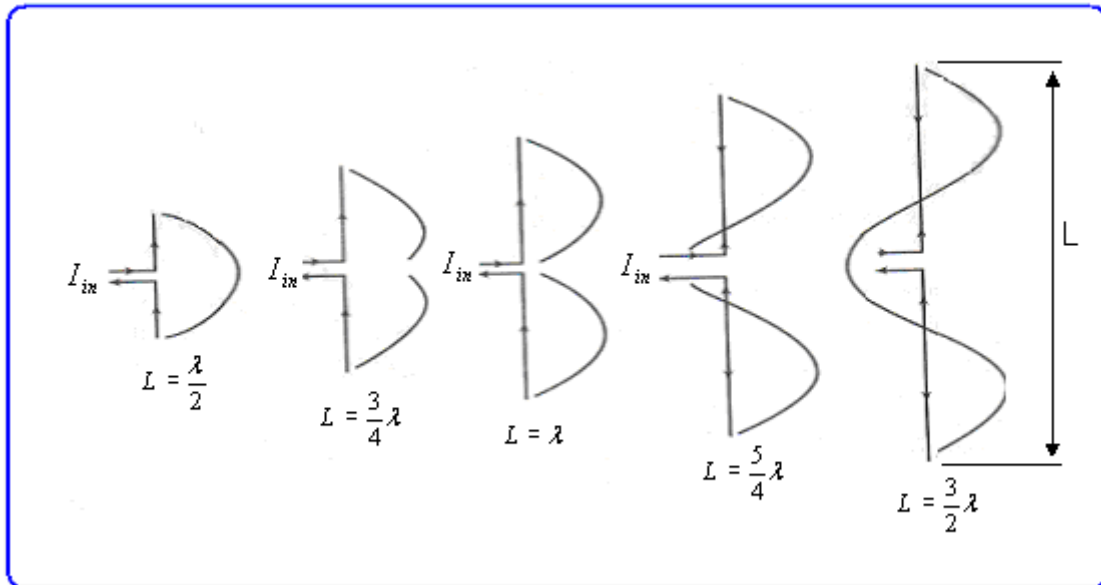


Figure 2.2: Current distribution on wire antenna with different lengths

The sinusoidal distributions of current and voltage are approximations rather than exact descriptions (Richmond, and Wang, 1974). They are slightly modified, on an actual antenna, by the radiation resistance of the antenna and by the fact that the antenna wires are not equivalent to a uniform transmission line. But the sinusoidal approximation is quite good for linear antenna whose conductors are very thin as compared to their length, and of high conductivity. It is assumed that the antenna wire is not close to any large irregular conducting bodies or dielectric material that would disturb the uniformity of the electrical environment. In fact, a free space environment is assumed, but the assumed distributions apply reasonably well in practical situations (Marsh, 1951; Mei, 1965; Miller et al., 1975; Poggio, 1987; Orfanidis, 2004). It was reported that sinusoidal current assumption frequently has an error in input impedance, which is approximately 1% for different antenna lengths (Stevenson, 1948; Wilton et al., 1976).

The problem of sinusoidal current assumption and its approximation can be addressed using the formulated equations by measuring the current distribution on full wave antenna and predicting the wave form shape using curve fitting in the manner, similar to Willard (1959) and Orfanidis (2004). In this study, formulae for the current distribution were obtained, and are based on measuring the current distribution on the full-wave dipole antenna.

Most of the previous works dealt with solutions to the integral equations given by Hallen as well as Pocklington. King (1967); King et al. (1967), carried out numerous theoretical and experimental studies on various cylindrical wire antennas by seeking analytical solutions to the integral equation following the pioneering work by Hallen (1938). A numerical technique based on the moment method (Mei, 1965; Werner, 1998) quickly become popular for analyzing radiation from a variety of wire antennas. The thin-wire approximation in the integral kernel was usually invoked in most moment method solutions.

Orfanidis (2004) showed that the equations above (Equation 2.1 to 2.8) were built on assumption and they were only an approximation, and they were not the exact form of the current distribution on linear antenna. He conducted his study in order to find exact equations of the current distribution instead of sinusoidal assumption. He expanded the solution of the current distribution. He used Hallen's equation, then he applied the sinusoidal approximation on Hallen's equation, and he got an approximate solution for the current distribution for the linear antenna. Based on Figure 2.3, he showed that Equation 2.10 is the basic form for determining the current on a center-fed linear antenna. He also

considered numerical approximate solution on it as well as numerical solution based on Moment's Methods (Orfanidis 2004).

$$\int_{-h}^h Z(z-z')I(z')dz' = v(z) = C_1 \cos \beta z + V_o \sin \beta |z| \quad 2.10$$

The solution of Equation 2.10 gives Equation 2.11, which is the standing-wave expression for the current

$$I(z) = I(0) \frac{\sin \beta(h-|z|)}{\sin \beta h}, I(0) = \frac{V_o \sin \beta h}{Z \cos \beta h} \quad 2.11$$

Where C_1 is a constant, and is determined from the end conditions $I(\frac{L}{2}) = I(-\frac{L}{2}) = 0$, and this shows that $I(z)$ is approximately

sinusoidal. The constant C_1 is fixed by the end-condition $I(\frac{L}{2}) = 0$, which gives:

$$C_1 = -V_o \frac{\sin \beta h}{\cos \beta h}, \quad \beta \text{ is the phase constant, } \beta = \frac{2\pi}{\lambda}, \lambda \text{ is wavelength in meter, } L$$

is the length of the antenna element, V_o is the input voltage at $z=0$, $h = \frac{L}{2}$, I_o is the input current at $z=0$, a is the radius of the wire, r is the distance from any point on the source to the observation point, (x,y,z) represents the observation point coordinates, and (x',y',z') represents the coordinates of the source.

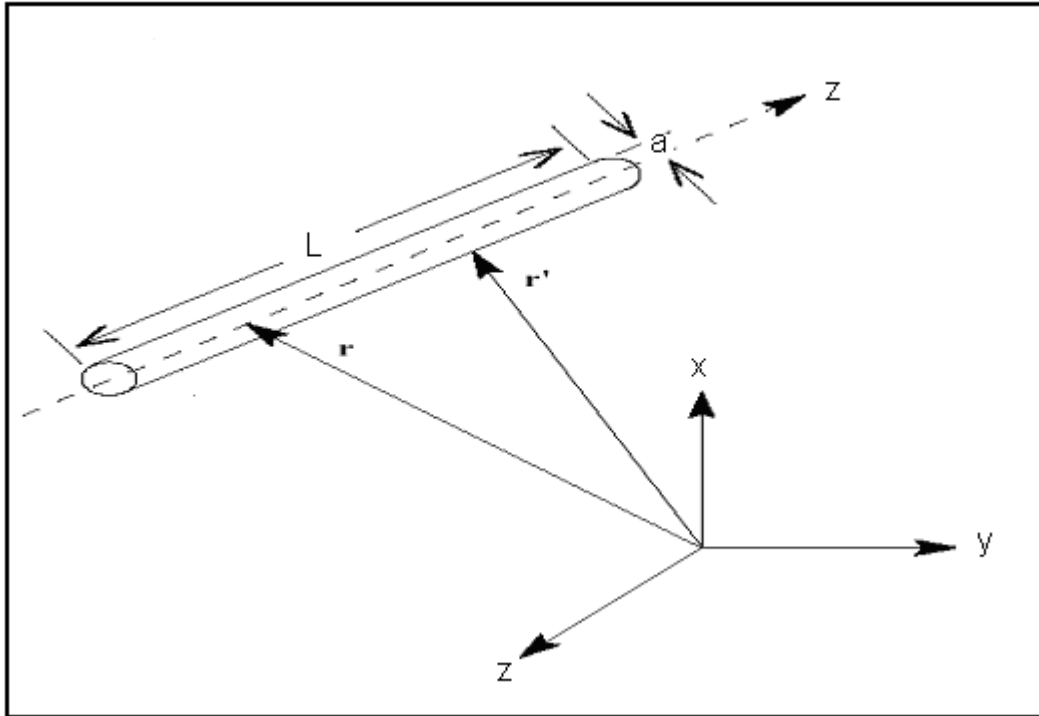


Figure 2.3: Thin wire model for linear antenna (Orfanidis 2004)

In (2004), he refined Equation 2.10, and used King's Three-Term Approximation. However, he showed that current distribution is a combination of sinusoidal and cosinusoidal terms as shown in Equation 2.12.

$$I(z) = \sin \beta |z| - \sin \beta h + \cos \beta z - \cos \beta h + \cos \beta \left(\frac{z}{2}\right) - \cos \beta \left(\frac{h}{2}\right) \quad 2.12$$

The current distribution for full wave antenna is based on the approximation of Hallen's solution and is depicted in Equation 2.13.

$$I(z) = \cos \beta h - \cos \beta z \quad 2.13$$

Wilton and Butler (1976) showed that Hallen formulation with point matching is equivalent to the Pocklington formulation with piecewise sinusoidal testing

functions. Caswell and Davis (1998) stated that Hallen's formulation is not as common as Pocklington's equation because it is more difficult to generalize for bent wire structures and will not be pursued any further. Figure 2.4 shows Hallen's solution, King's approximation and sinusoidal approximation of the current distribution on linear antenna.

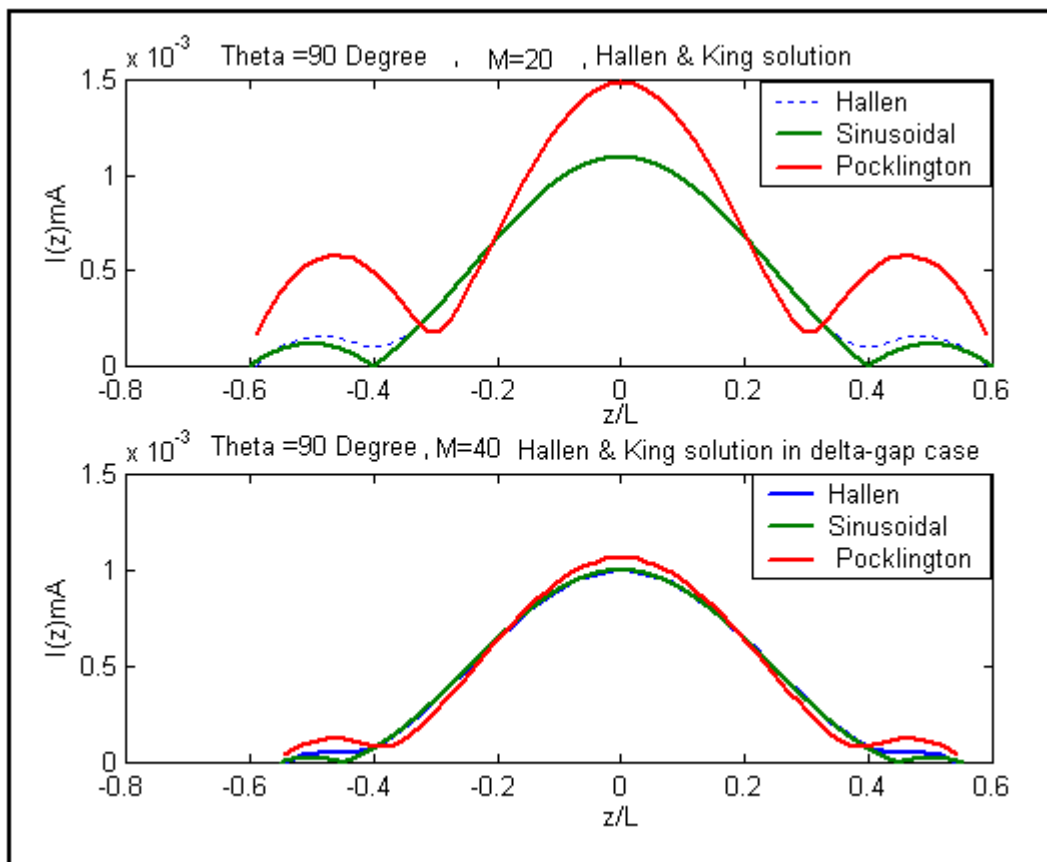


Figure 2.4: Current distribution on linear antenna (Orfanidis 2004)

Vinoy (2002) formulated an equation for the current distribution on linear antenna. He used Hallen's equation and he didn't consider the effect of end faces, and the currents at $z = \pm L$ were taken as equal to zero. His formula is depicted in Equation 2.14. He obtained the current distribution in terms of the

antenna dimensions and the impedance (due to skin effect (Anderson, 1985)) of the conductor as shown in Figure 2.5 (Vinoy 2002).

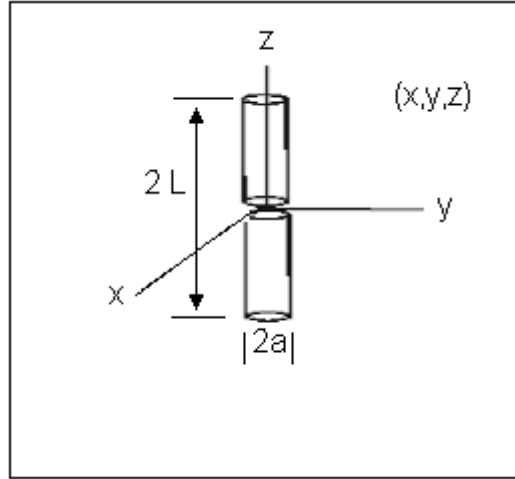


Figure 2.5: Geometry of Cylindrical Dipole Antenna

$$I(z) = \frac{jV_{in}}{120 \ln \frac{2L}{a}} \left[\frac{2 \ln \frac{2L}{a} \sin \beta(L - |z|) + b_1}{2 \ln \frac{2L}{a} \cos \beta L + d_1} \right] \quad 2.14$$

Where,

$$b_1 = F_1(z) \sin \beta L - F_1(L) \sin \beta |z| + G_1(L) \cos \beta z - G_1(z) \cos \beta L \quad 2.15$$

$$d_1 = F_1(L) = \int_{-1}^1 \frac{(\cos \beta z_1 - \cos \beta L)}{r} e^{-j\beta r_1} dz \quad 2.16$$

$$F_1(z) = F_{0z} \ln \left[1 - \left(\frac{z}{L} \right)^2 \right] + F_{0z} \ln \left[\frac{1}{4} \left\{ \sqrt{1 + \left(\frac{a}{1-z} \right)^2} + 1 \right\} \right] \left[\sqrt{1 + \left(\frac{a}{1+z} \right)^2} + 1 \right]$$

$$- \int_{-1}^1 \frac{F_{0z} e^{-j\beta r} - F_{0z}}{r} dz \quad 2.17$$

$$G_{0z} = \sin \beta |z| - \sin \beta L \quad 2.18$$

$$F_{0z} = \cos \beta z - \cos \beta L \quad 2.19$$

β is the phase constant, $\beta = \frac{2\pi}{\lambda}$, λ is wavelength in meter, L is the length of the antenna element, a is the radius of the wire, r is the distance from any point on the source to the observation point, (x,y,z) represents the observation point coordinates, and (x',y',z') represents the coordinates of the source.

Storm (1952) obtained an approximate solution to Hallen's integral equation by expanding the current distribution in Fourier series of the normal current mode of the antenna, using symmetry and boundary conditions that $I_z(\pm h) = 0$, (where h is the length of the antenna), the current distribution is indicated in Equation 2.20.

$$I(z) = A \sin \beta(h - |z|) + \sum_n A_n \cos k_n z \quad 2.20$$

Where, A and A_n are complex coefficients, $k_n = \frac{n\pi}{2h}$.

Rusch (1959) conducted a research on full wave antenna. Using matrix solution of linear antenna with loading, he assumed that the radius of the wire antenna must be extremely small as compared to the length, and the current at the end of the antenna is assumed to be zero. In the manner similar to storm, he expanded the axially-directed current in Fourier Series, to derive an equation of the current distribution for full wave antenna as shown in Equation 2.21.

$$I(z) = \sum_{n=1}^{\infty} I_n \sin k_n (z + a_n) \quad 2.21$$

Where $kn = \frac{n\pi}{2h}$, and $an = \frac{n\pi}{2}$.

He validated Equation 2.21 for antenna with asymmetrical feed and asymmetrical loading, dropping the subscript z from the current notation as the symmetry about z is equal to 0. He reformulated Equation 2.21 to Equation 2.22 in order to obtain an equation for a symmetrical feeding and specific pure real loading impedance.

$$I_n = I_o \sin \frac{n\pi}{2} \quad 2.22$$

Equation 2.22 is valid for any general number and location of feed points and any arbitrary nature and distribution of loading elements. Figure 2.6 shows the current distribution on full wave antenna calculated by King's approximation, and matrix methods (Willard Rusch, 1959).

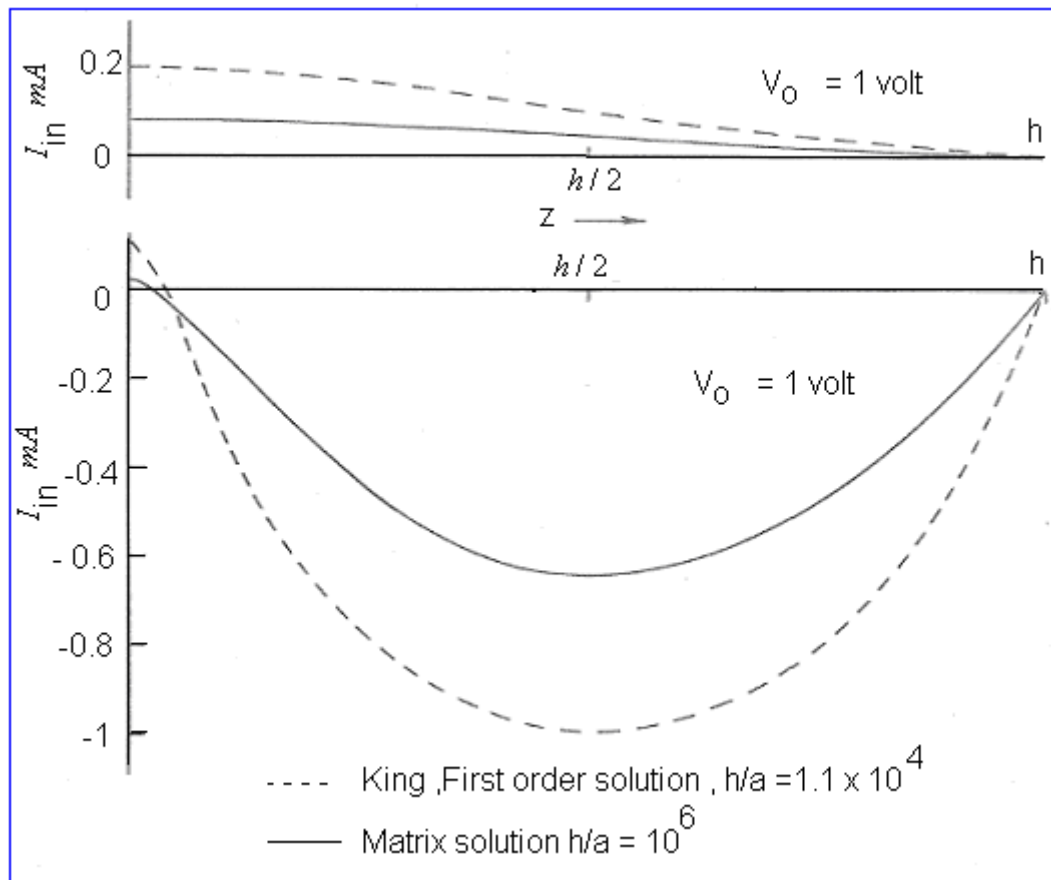


Figure 2.6: Comparison of real and imaginary current distributions on full-wave unloaded antenna calculated by King's approximation and matrix methods (Rusch, 1959)

Tsai (1972); Dyson (1973); Smith (1981); Hassan (1987); Idris et al (1999) have shown that the measurement of the current distribution using a shielded loop, protruding through a slit in the antenna surface along its axis, gives exact and accurate measurement rather than sinusoidal approximation .

Shigeru et al. (1981) and Egashira, et al. (1985) have measured the current distribution by moving a shielded loop near a test antenna along its axis so that the distance between the test antenna and the shielded loop are lesser than

both the length of the test antenna and the wavelength. Edwards (1963); King et al (1981); Whiteside et al (1963) have also carried out the research in connection with the measurement using a shielded loop. King et al (1981) expressed the EMF on the loop projecting through a slot in the metal surface in terms of contributions from the magnetic field, the electric field, and the derivatives of electric field.

Edwards (1963) described the method of measurement with a shielded loop located outside the test antenna, and Whiteside et al (1963), studied the current estimation of the property of the loop. However, in the former the relation between the measured value and the current distribution was not investigated (Shigeru, 1988). This method may be used when the radius of the dipole is rather thick. Thus, if a wire is thick, one can easily measure the current distribution by moving a shielded loop near a test antenna and along its axis (Libby, 1946; Whiteside & King, 1964; Hassan, 1987; Shigeru, 1988; Idris et al., 1994; Idris et al., 1999).

Tang and Gunn (1981) stated that the current distribution along a receiving dipole antenna depends greatly on the load (Z_L). They also stated that under mismatch conditions, the current distribution can change significantly and the sinusoidal approximations is no longer valid, and the equation of the current distribution may be given as:

$$I(z) = V_{20}v(z) + U_{21}u(z) \quad 2.23$$

Where $v(z)$ is associated with virtual voltage source V_{20} at the antenna feed point, and $u(z)$ is related to the charge distribution throughout the antenna elements. U_{21} is the function of incident electric field.

2.2 Feed Mechanisms for Full-Wave Dipole Antenna

Selection of the feeding technique is governed by several factors, the most important of which is the consideration of efficient power transfer from the feed structure to the radiating structure. There are mainly seven configurations used in this study to feed the full-wave dipole antenna.

2.2.1 Center-Fed Dipole Antenna

A center-fed electrical dipole antenna is illustrated in Figure 2.7(A). The current on a dipole antenna, as illustrated in Figure 2.7(B) is sinusoidal, if the diameter of the wire ($d = 2a$) is much less than the wavelength (Uchida & Mushiake, 1970).

The current is maximum at the feed point if the dipole is operated below resonance ($L < \lambda/2$), and must fall to zero at the ends of the wire. As the current magnitude decreases, charges peel off and appear on the surface of the wire as illustrated in Figure 2.7(A). These charges lead to a displacement current in the free space surrounding the dipole. The varying displacement current produces an outwardly propagating electromagnetic wave (Stutzman, 1981; Tam & Robert, 1987; Tam, et al.1987; Junker et al., 1995). The length of an electrical small dipole antenna is much less than a half wavelength ($L \ll \lambda / 2$). Thus, an electrical small antenna is operated below resonance and the current must go

to zero at the ends of the dipole, regardless of antenna length (Stutzman et al., 1981; Saoudy & Sinha, 1990; Dietrich et al., 1997).

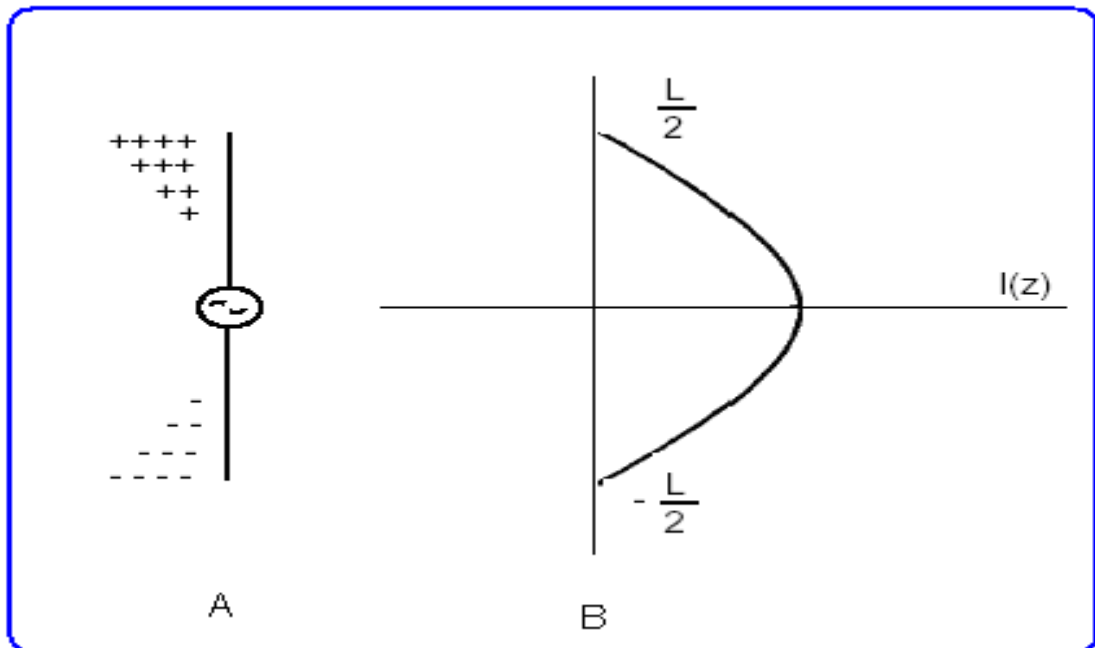


Figure 2.7: (A) a center-fed dipole antenna, (B) The Current Distribution along the length of the Dipole

Wheeler (1947) pointed out that a true electric dipole is equivalent to two equal and opposite polarity point charges separated by a definite distance. In this sense, the elemental dipole and the short dipole are equivalent to oscillating electric dipole. If the length of antenna is substantially greater than a half wavelength it is classified as long-wire antenna, and is not properly called dipole. Although the half-wave antenna is commonly called a half-wave dipole yet, there is a doubt about the propriety of this nomenclature.

Varadan et al (1995) have shown that a center-fed half-wave dipole consisting of a straight wire, one-half wavelength long and fed in the center while a center-

fed dipole can be of any length electrically, as long as it is configured in a symmetrical fashion with two equal-length legs. In general the greater in the length of a center-fed antenna, in terms of wavelength, the larger the number of lobes into which the pattern splits. A feature of all such patterns is the fact that the main lobe - the one that gives the largest field strength at a given distance - always is the one that makes the smallest angle with the antenna wire. Furthermore, this angle becomes smaller as the length of the antenna is increased.

Idris et al. (1994) showed that the full wave dipole antenna is seldom used in communication system, and yet this type of antenna offers a very high gain if feeding is devised properly. He indicated that by feeding the antenna in the center-tap, it introduces excessively high impedance due to low current at the antenna. Hassan (1987) managed to reduce the input impedance from 800 Ω to 50 Ω using a thick wire rather than thin one, and he showed that the thick wire is more efficient regarding the radiation due to current flowing on the surface of the wire. However, his study was conducted for matching purpose. Johnston and McRory (1998) have shown that the larger diameter wires have a measurably higher efficiency than a thinner wire.

Georgieva (2005) constructed an array of 4 in-phases $\frac{1}{2}\lambda$ -elements with a center single-feed, by means of tuned traps. Each trap represents a tuned parallel LC circuit as shown in Figure 2.8 and 2.9. It was also shown that this type of antenna achieved a gain of 6.4 dBi.

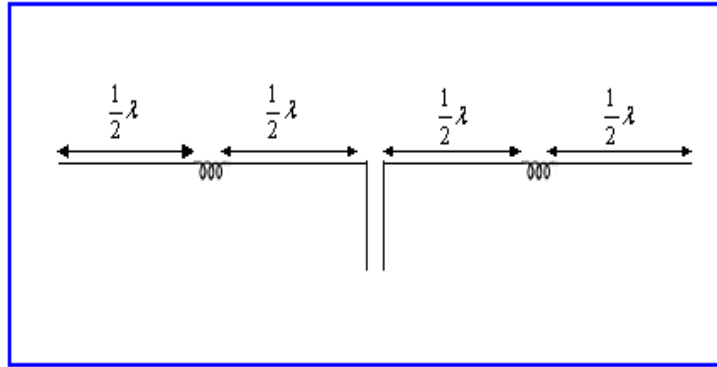


Figure 2.8: Dipole antenna with trap

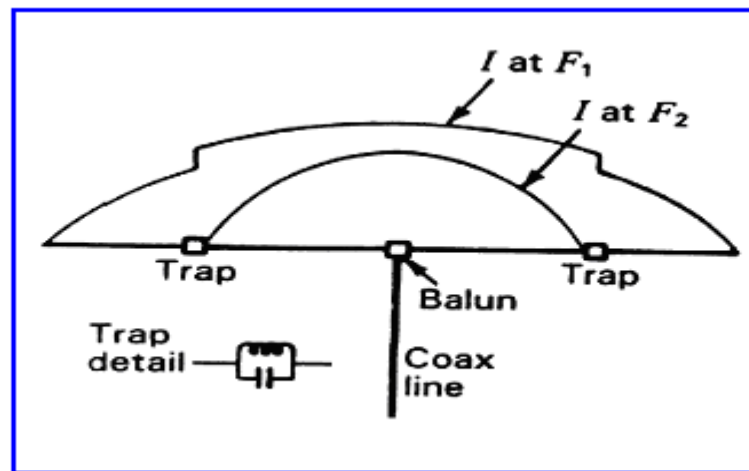


Figure 2.9: Current distributions for wire antenna with traps

The full wave antenna with different types of feeding was studied quite thoroughly with the aim of improving the gain of the full wave dipole antenna in the manner similar to Georgieva (2005). An improvement of about 6 dB was achieved. However, this increase in directivity is at the cost of increasing the number of feeding points of the antenna. This antenna could provide directivity more than 6 dB if the feeding were to be designed using more sophisticated equipment under highly controlled environmental conditions. In fact, under the current measurement conditions the percentage of error (Refer to Appendix A) is supposed to be about 20% according to IEEE and standard books (Pozar & Kaufman, 1988; Johnston et al., 1996; Johnston & McRory, 1998; David, 1998;

Shafai, 1998; Lewellyn, 1998). Shafai (1998) performed the measurements in anechoic chamber, where a measurement repeatability of 0.25 dB is obtainable, and their reference gain horn is specified at an accuracy of 0.5 dB and that translated into an accuracy of +19% and -16% on a high-efficiency antenna (Johnston & McRory, 1998).

2.2.2 Off-Center Fed Dipole Antenna

The off-center feed arrangement is unsymmetrical and can lead to undesirable phase reversals in the antenna. As the feed point approaches the end of the wire the resistance approaches infinity. In practice, the input resistance becomes very large as the feed point moves out. The pattern essentially unchanged as the feed point shifted (King & Smith, 1981; Idris et al 1999; Rowe & Waterhouse, 2000; Georgieva 2005).

For longer dipole, the pattern and impedance differ significantly from the center-fed case as the feed point is displaced. For example, a full-wave dipole fed a quarter-wavelength from one end, as shown Figure 2.10(A) will have a current distribution that is significantly different from center fed full wave dipole as shown in Figure 2.10(B) (Wheeler, 1947; Harrington, 1960; Vinoy et al, 2001; Vinoy et al., 2002).

Stutzman et al (1981) showed that the asymmetric feed positioning is often used for linear dipole antennas, and in such a case the current at the new input terminals is depicted in Equation 2.24.